

Biofunctionalization of Metal–Organic Framework Nanoparticles via Combined Nitroxide-Mediated Polymerization and Nitroxide Exchange Reaction

Ilona Wagner, Simon Spiegel, Julian Brückel, Matthias Schwotzer, Alexander Welle, Martina H. Stenzel, Stefan Bräse, Salma Begum,* and Manuel Tsotsalas*


Surface engineering of metal–organic framework nanoparticles (MOF NPs), and enabling their post-synthetic modulation that facilitates the formation of bio-interfaces has tremendous potential for diverse applications including therapeutics, imaging, biosensing, and drug-delivery systems. Despite the progress in MOF NPs synthesis, colloidal stability and homogeneous dispersity—a desirable property for biotechnological applications, stands as a critical obstacle and remains a challenging task. In this report, dynamic surfaces modification of MOF NPs with polyethylene glycol (PEG) polymer is described using grafting-from PEGylation by employing nitroxide-mediated polymerization (NMP) and inserting arginylglycylaspartic acid (RGD) peptides on the surface via a nitroxide exchange reaction (NER). The dynamic modification strategy enables tailoring PEG-grafted MOF NPs of the type UiO-66-NH₂ with improved colloidal stability, and high dispersity, while the morphology and lattice crystallinity are strictly preserved. The interaction of PEG-grafted MOF NPs with human serum albumin (HSA) protein under physiological conditions is studied. The PEG-grafted colloidal MOF NPs adsorb less HSA protein than the uncoated ones. Therefore, the described approach increases the scope of bio-relevant applications of colloidal MOF NPs by reducing nonspecific interactions using NMP based PEGylation, while preserving the possibility to introduce targeting moieties via NER for specific interactions.

1. Introduction

Nanoparticles of metal–organic frameworks (MOF NPs) are an emerging class of porous modular materials, feature well-defined crystalline structure, intrinsic porosity with narrow pore size distribution and amenable to post-synthetic modification (PSM) for grafting specific functionalities and desired properties.^[1–6] MOF NPs have been investigated for many bio-relevant applications including therapeutics, imaging, biosensing, and drug-delivery systems.^[7–9] In many of the before mentioned applications, surface chemistry modulation of MOF NPs has been of fundamental relevance and a crucial factor in interactions with the surrounding media.^[10,11] For tailoring novel MOF NPs, various strategies including post-synthetic modification of the MOF NPs via coordinative functionalization at the metal/cluster nodes and covalent modification within the molecular skeleton have been demonstrated.^[11,12] For instance, colloidal crystal engineering of MOF NPs with oligonucleotides,^[13] coordinative surface functionalization of MOF NPs with polymers of bio-relevance,^[14] and surface-selective covalent attachment of polymers to MOF

I. Wagner, S. Spiegel, M. Schwotzer, A. Welle, S. Begum, M. Tsotsalas
Institute of Functional Interfaces (IFG)
Karlsruhe Institute of Technology (KIT)
Hermann-von Helmholtz-Platz 1, 76344 Eggenstein-Leopoldshafen,
Germany
E-mail: salma.begum@kit.edu; manuel.tsotsalas@kit.edu

J. Brückel, S. Bräse
Institute for Organic Chemistry (IOC), Karlsruhe Institute of Technology (KIT)
Fritz-Haber-Weg 6
76131 Karlsruhe, Germany
A. Welle
Karlsruhe Nano Micro Facility, Karlsruhe Institute of Technology (KIT)
Hermann-von-Helmholtz-Platz 1
76344 Eggenstein-Leopoldshafen, Germany
M. H. Stenzel, S. Begum
Center for Advanced Macromolecular Design, School of Chemistry
University of New South Wales
Sydney, NSW 2052, Australia
S. Bräse
Institute of Biological and Chemical Systems - Functional Molecular Systems (IBCS-FMS), Karlsruhe Institute of Technology
Hermann-von-Helmholtz-Platz 1
76344 Eggenstein-Leopoldshafen, Germany

 The ORCID identification number(s) for the author(s) of this article can be found under <https://doi.org/10.1002/mame.202300048>

© 2023 The Authors. Macromolecular Materials and Engineering published by Wiley-VCH GmbH. This is an open access article under the terms of the Creative Commons Attribution License, which permits use, distribution and reproduction in any medium, provided the original work is properly cited.

DOI: 10.1002/mame.202300048

NPs have been accomplished.^[15,16] Other elegant strategies for grafting polymers to develop functional MOF NPs have been reported for applications in (bio)technologies.^[17] However, despite the progress in MOF NPs synthesis, colloidal stability and homogeneous dispersity stands as a critical obstacle that offer the opportunity for certain improvements to avoid aggregation of MOF NPs suspensions.^[18,19] In this vein, introducing a rather different approach, we have established dynamic surface modification of MOF NPs employing post-synthetic nitroxide-mediated polymerization (NMP) via alkoxyamine functional groups.^[20] In this report, we demonstrate external surface modification of MOF NPs of the type UiO-66-NH₂ with dynamic alkoxyamines that serve as initiators to grow polymers via post-synthetic NMP approach using a PEO-methyl-p-vinylbenzyl-ether (SPEGA) as monomer. Literature known procedures for grafting *from*- the MOF surface often feature atom transfer radical polymerization and hydrophobic polymers, such as poly(methyl methacrylat) (PMMA).^[21] By employing both NMP and nitroxide exchange reaction (NER) furnish polyethylene glycol (PEG)-grafted MOF NPs with improved colloidal stability, enhanced coagulation time in aqua media, and high dispersity, while preserving the possibility of polymer chain end functionalization with proteins and other biomolecules. We have demonstrated that the PEG-grafted colloidal MOF NPs adsorb less human serum albumin (HSA) protein than the uncoated ones, thus, increase the scope of bio-relevant applications of colloidal biomolecular MOF NPs.

2. Results and Discussion

2.1. MOF Nanoparticle Surface Modification

Grafting synthetic polymers on the surfaces of MOFs is a versatile approach and, in general, carried by two methods, namely grafting *from*- and grafting *to*- reaction.^[22] In the grafting *from*-method, MOFs can be decorated with initiating sites on the surface from where polymerization starts, while in the grafting *to*-approach, the pre-synthesized polymer in bulk is grafted via an anchoring functional group *to*- the surface. The pre-synthesized polymers advantage is the polymer's easier characterization in advance, but it suffers from the low grafting density. In contrast, *from*- the surface synthesis strategy could be difficult in characterization since most techniques require the cleavage and isolation of the polymer from the surface. Nevertheless, the advantage of the grafting *from*- method is the high density of polymer tailoring on the surface.^[22,23] Alkoxyamines that contain a thermo-labile C-ON bond combine the ability to dynamically break, form, and reform covalent bonds with the possibility to initiate reversible-deactivation radical polymerization.^[24,25] Alkoxyamines on thermal homolysis generate persistent nitroxide radicals that can be used for reversible nitroxide-exchange reactions in the presence of an additional nitroxide radical species or initiate a controlled polymerization of NMP process by monomer addition. Being able to avoid additional mediators or the need for catalyst removal and potential contamination by metals or thiol-based components, favors the use of NMP applying grafting *from*- method, especially for biological applications, as it is triggered by temperature and needs no further purification.^[26] The reactivity of alkoxyamines and subsequent polymerization process can be controlled precisely through the molecular design of

the nitroxides.^[27] Employing this dynamic strategy, details and sequence for our designed concept for surface modification of MOF NPs via post-synthetic NMP is depicted in **Figure 1**.

Applying our previously reported surface modification procedure for UiO-66-NH₂ using alkoxyamines,^[20] we used polyethylene glycol, more precisely PEO-methyl-p-vinylbenzyl-ether (referred here to as SPEGA) in NMP to graft PEG polymer on the surfaces of the MOF NPs. Surface modification of UiO-66-NH₂ with 2,2,6,6-Tetramethylpiperidinyloxy (TEMPO)-alkoxyamine (AA) was performed via amide bond formation using (3-Dimethylamino-propyl)-ethyl-carbodiimide hydrochloride/N-hydroxysulfosuccinimid (EDC/sulfo-NHS), followed by controlled NMP free radical polymerization of SPEGA. The SPEGA polymerization initiated from the pre-attached alkoxyamine units on the UiO-66-NH₂, the overall reaction scheme is represented in **Figure 2A**. Successful attachment of the alkoxyamine functions and successive surface PEGylation while preserving the pristine MOF crystallinity intact, was confirmed by Attenuated Total Reflection Infrared Spectroscopy (ATR-IR), Time-of-Flight Secondary Ion Mass Spectrometry (ToF-SIMS) and Powder X-ray diffraction (PXRD) characterization methods (**Figure 2**).

ATR-IR spectra of SPEGA polymer, pristine UiO-66-NH₂, and PEG functionalized UiO-66-NH-AA-SPEGA, are presented in **Figure 2B**. The appearance of new bands in the case of UiO-66-NH-AA-SPEGA in the area from 900 to 670 cm⁻¹, at 1100 and 2866 cm⁻¹, are attributed to the characteristic bands of PEG polymer. The band around 699 cm⁻¹ corresponds to the mono substituted benzene vibrations from SPEGA, while the typical O=C-O-C and C-H stretching vibration from the PEG polymers are observed at 1100 and 2866 cm⁻¹, respectively. ATR-IR spectra of UiO-66-NH-AA-SPEGA in comparison to the pristine UiO-66-NH₂ and the reference SPEGA monomers, confirms the existence of PEG polymers, and thus demonstrate the successful incorporation of SPEGA monomers on the alkoxyamine functionalized MOF NPs. ToF-SIMS data, normalized on the Zr-signal, provides further evidence for the existence of PEG polymer on SPEGA functionalized MOF NPs. PEG-related typical fragments at *m/z* 31.02 (CH₃O⁻), 43.02 (C₂H₃O⁻), and 59.05, (C₃H₇O⁻) are observed in PEG functionalized MOF NPs, whereas these signals are absent in pristine and alkoxyamine functionalized UiO-66-NH₂. Furthermore, PXRD patterns confirm the retention of the crystalline phase of MOF NPs after the surface modifications with AA and SPEGA. The pristine and modified UiO-66-NH₂ samples show the characteristic PXRD pattern of UiO-66-NH₂, and all patterns well match to the simulated pattern (**Figure 2D**).

2.2. Dispersion Stability and Protein Adsorption

The scanning electron microscope (SEM) images of the pristine (UiO-66-NH₂) and the modified MOF NPs (UiO-66-NH-AA and UiO-66-NH-AA-SPEGA) show octahedron crystals with the average crystal sizes of around 150 nm in diameter (**Figure 3A**). Modulating MOF NPs colloidal stability, homogeneous dispersity and to avoid aggregation of MOF NPs suspensions has been a crucial consideration. Reduced agglomeration tendency appears to be associated with the polymer composition and the polarity of the solvent media. During our previous investigations, we observed

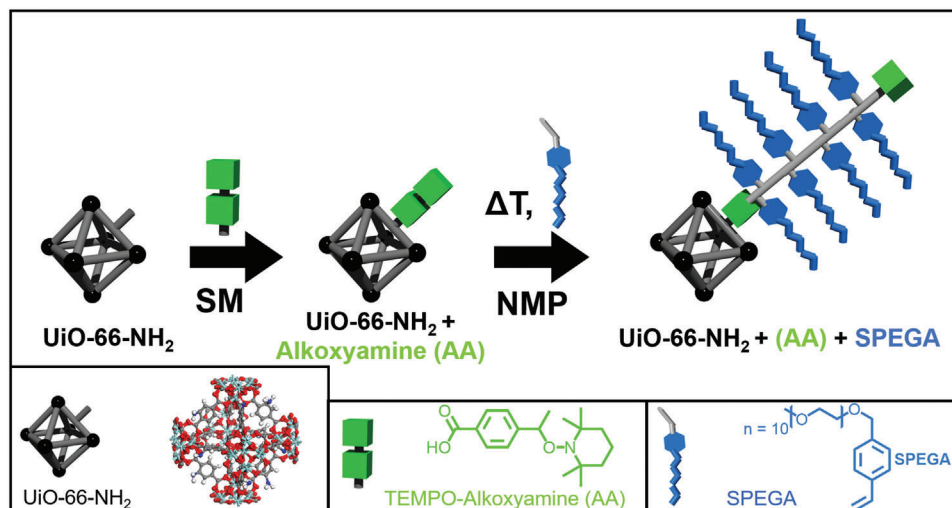


Figure 1. Schematic overview of the PEG grafting from the surface of UiO-66-NH₂ NPs via NMP. In the first surface modification (SM) step, 2,2,6,6-Tetramethylpiperidinyloxy (TEMPO)-alkoxyamine (AA) is attached to the pristine MOF NPs via amide bond formation. In the second step, AA serves as initiator for the NMP reaction, where AA is dynamically exchanging with PEO-methyl-p-vinylbenzyl-ether (SPEGA). After polymerization the alkoxyamine exchange function remains active.

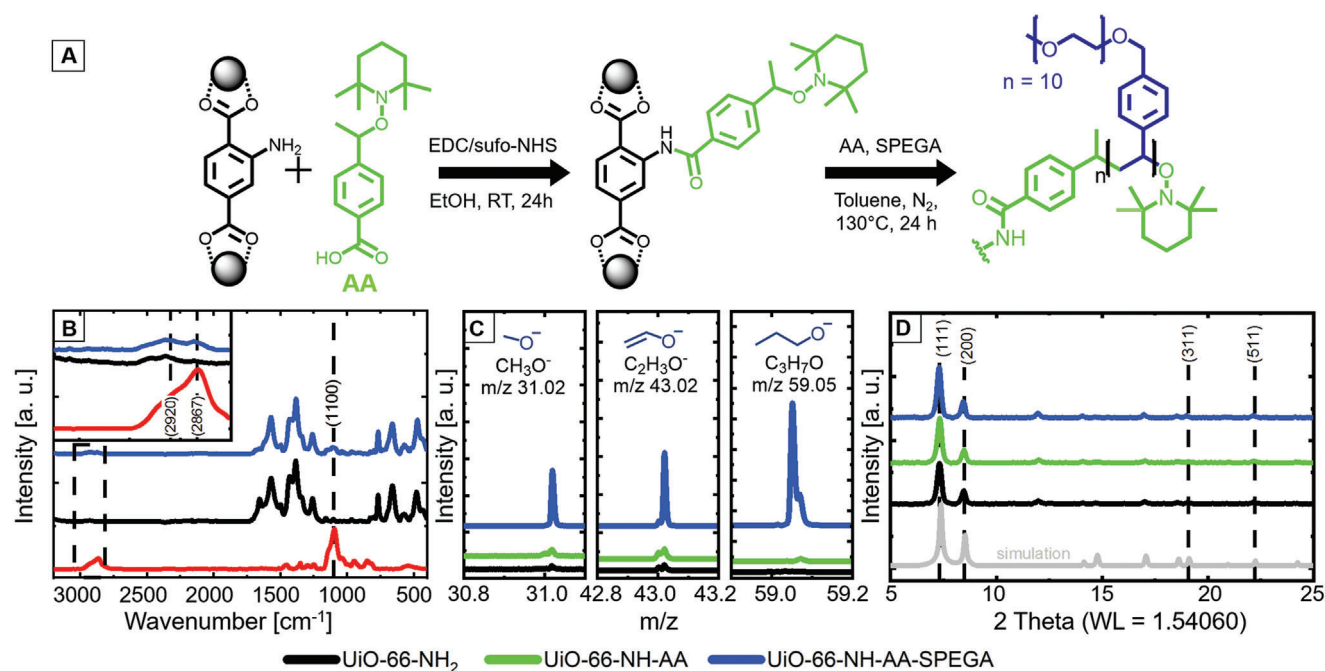


Figure 2. Overview of MOF NPs modifications. A) Reaction scheme of UiO-66-NH₂ successive surface modification with alkoxyamines and SPEGA, black spheres represent [Zr₆O₄(OH)₄]¹²⁺-cluster. Characterization of the pristine MOF UiO-66-NH₂ (black), the alkoxyamine-modified MOF UiO-66-NH₂ (green), SPEGA polymer (red), and SPEGA functionalized MOF UiO-66-NH-AA-SPEGA (blue) by B) ATR-IR; C) ToF-SIMS showing CH₃O⁻, C₂H₃O⁻ and C₃H₇O⁻ signals normalized on the Zr-signal and D) PXRD.

a decreased agglomeration tendency of polystyrene(PS)-modified MOF NPs in toluene.^[10] Similarly, the SPEGA-modified MOF NPs in this study demonstrate a reduced agglomeration and good dispersibility in ethanol (EtOH) and remain homogeneously distributed for days, while the pristine ones settle down in hours (Figure 3B). The MOF NPs showed a different aggregation tendency based on their surface modification (nonpolar

or polar polymer). While the PS-modified particles are more stable in nonpolar solvents, like toluene, the SPEGA-modified MOF NPs show less aggregation tendency in polar solvents, like EtOH, as shown in Figure 3B. The PEG chains grafted to the MOF NPs maintain a well-dispersed stable suspension of MOF NPs in EtOH and prevent the particles from agglomeration. Additionally, the dynamic light scattering (DLS) measurements

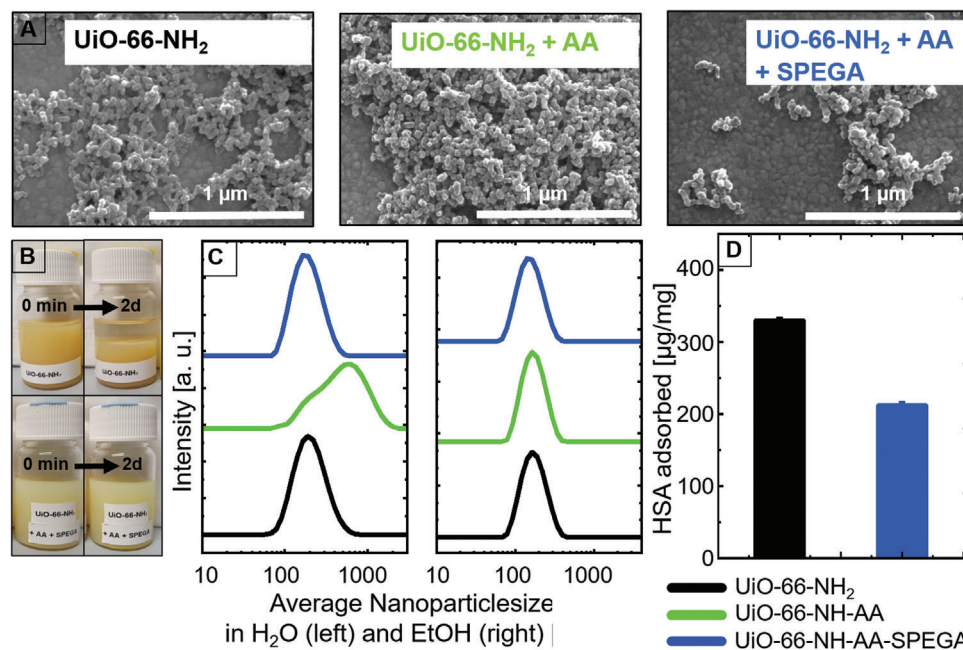


Figure 3. Characterization of MOF NPs size distribution before and after the surface modification by A) SEM analysis B) Optical images of pristine UiO-66-NH₂ (top) and SPEGA functionalized UiO-66-NH-AA-SPEGA NPs (bottom) suspended in EtOH: both samples are well dispersed at 0 min, pristine MOF NPs are settling down over time while the SPEGA functionalized MOF NPs remain well suspended over 2 d. C) DLS size distribution measurements in water and EtOH; UiO-66-NH₂ (black), UiO-66-NH-AA (green), and UiO-66-NH-AA-SPEGA (blue). D) HSA adsorption by pristine UiO-66-NH₂ (black), and SPEGA-modified MOF NPs (blue) after 4 h incubation at 37 °C, assayed by BCA assay.

(Figure 3C) show a narrow particle size distribution for the SPEGA-modified NPs. In water, the particle size was around 195 ± 63.7 nm for the pristine MOF and 191 ± 73.3 nm for the SPEGA-modified MOF NPs. In EtOH, the SPEGA-modified MOF NPs show lower particle sizes (163 nm \pm 55.0 nm) compared to the pristine MOF NPs (177 ± 54.5 nm). In comparison to the SPEGA-modified MOF NPs, the alkoxyamine-modified MOF NPs in water show a wide range of large particle size distribution (two peaks around 761 ± 359 nm and 236 ± 66.6 nm).

We used PEGylation of UiO-66-NH₂ to modulate their colloidal stability and homogeneous dispersity with features preventing their recognition and clearance by the innate immune system, a required trait for biomedical applications. Reducing the non-specific protein adsorption on drug carrier systems is a valuable feature to enhance the blood circulation time and the effectiveness of the drug nanocarriers. To gain insight on the influence of SPEGA functionalized MOF NPs on protein adsorption under physiological conditions, human serum albumin (HSA), the most abundant protein in human blood plasma, was chosen for this study. Pristine and SPEGA functionalized MOF NPs were incubated for 4 h at 37 °C in an ammonium acetate solution containing HSA. After centrifugation, the amounts of non-adsorbed HSA in supernatants were quantified using a bicinchoninic acid (BCA) titration assay. The amount of adsorbed protein on pristine UiO-66-NH₂ NPs ($329 \mu\text{g mg}^{-1} \pm 4.20$) and UiO-66-NH-AA-SPEGA ($211 \mu\text{g mg}^{-1} \pm 4.90$) modified NPs is shown in Figure 3D. This demonstrate that the SPEGA-grafted colloidal MOF NPs adsorb less HSA protein than the uncoated ones, thus, increase the scope of bio-relevant applications of colloidal MOF NPs.

2.3. Nitroxide End-Group Exchange - Post-fabricated RGD Grafting on PEGylated MOF NPs

Nitroxide-exchange reaction (NER) is a favourable tool to modify the polymerization chain via nitroxide end-group exchange.^[28,29] The nitroxide end-group on polymers enable further modification of the MOF NPs and diverse functional moieties desired for specific functions can be incorporated in a highly controlled way. We have shown nitroxide exchange reaction of TEMPO with the nitroxide (2-lambda1-oxidanyl-1,1,3,3-tetramethylisindole, known as TMIIO).^[20,30] We evaluated this possibility by attaching a tumor targeting RGD-sequence (Figure 4A) to the polymer via a nitroxide-exchange reaction. RGD is an amino acid sequence consisting of a Arg-Gly-Asp peptide first described in 1970.^[31] The exchange of the TEMPO group on the SPEGA-modified MOF NPs with the RGD-nitroxide was confirmed by ToF-SIMS.

A clearly visible intense signal of TEMPO⁺ observed at m/z 156.14 before the NER in UiO-66-NH-AA-SPEGA, is significantly reduce after the exchange reaction in the sample labeled as UiO-66-NH-AA-SPEGA-RGD. Significant difference in the TEMPO⁺ signal was observed for UiO-66-NH-AA-SPEGA before and after the RGD grafting via NER, confirming the successful and complete exchange of the TEMPO end-group with the RGD-sequence. In addition, the representative fragments of the RGD sequence, such as typical signals for arginine around m/z 43.03, 100.09, and 127.10 are observed (Figure 4B). Presence of arginine signals and absence of the intact RGD signal (m/z 642.3) in UiO-66-NH-AA-SPEGA-RGD NPs further confirms that the RGD-sequence is successfully attached to the MOF NPs via a covalent bond and rule out the presence of physisorbed RGD molecules.

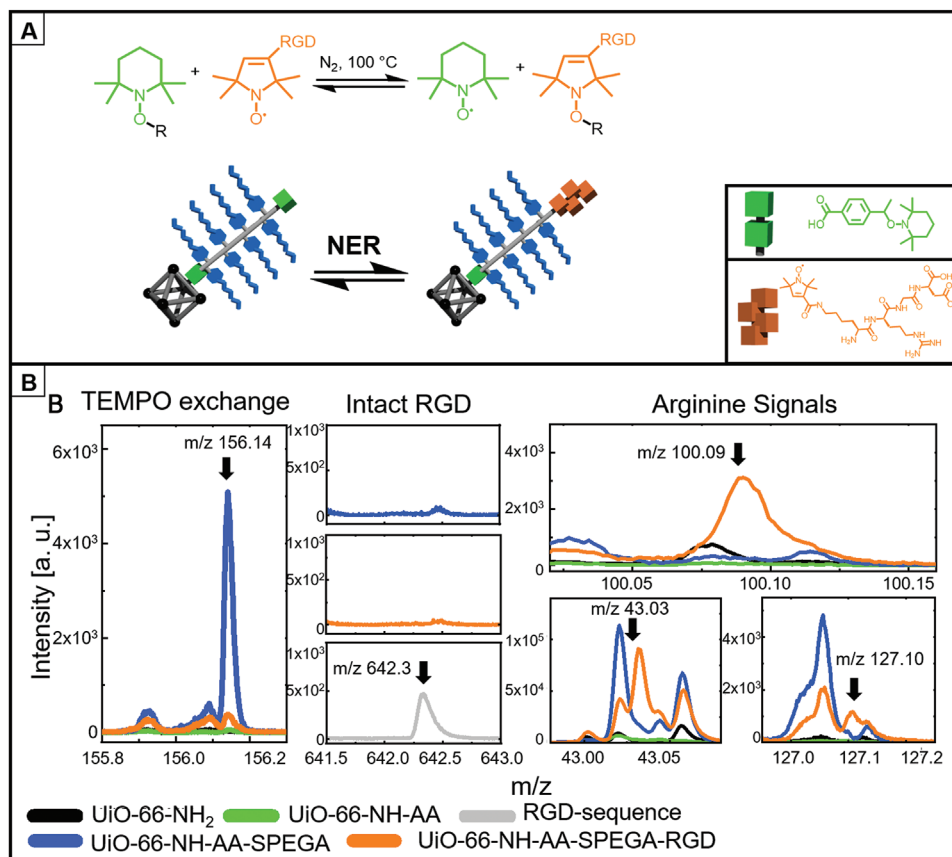


Figure 4. Nitroxide exchange reaction (NER) of UiO-66-NH-AA-SPEGA with RGD-nitroxide A) scheme of the exchange process. B) ToF-SIMS showing TEMPO+, intact RGD-nitroxide and arginine signals in pristine UiO-66-NH₂ (black), Alkoxyamine functionalized UiO-66-NH-AA (green), PEG functionalized UiO-66-NH-AA-SPEGA before (blue) and after NER with RGD-nitroxide UiO-66-NH-AA-SPEGA-RGD (orange).

3. Conclusion

As the size and morphology of UiO-66-NH₂ MOF particles can be precisely controlled, while modulating colloidal stability and homogeneous dispersity has been a desirable property for bio-relevant applications. In this vein, we developed a covalent modification strategy for controlled grafting polymers from the surface of MOF NPs via nitroxide-mediated polymerization. This strategy enables tailoring surface properties of MOF NPs with improved colloidal stability, and high dispersity while preserving crystallinity and particles size. In proof-of-concept study, we have demonstrated that the PEG-grafted colloidal MOF NPs adsorb less human serum albumin protein than the uncoated ones, thus, increase the application scope of colloidal biomolecular MOF NPs. Additionally, a broad range of biomolecules, proteins, antibodies, and fluorescent moieties can be introduced in a precisely controlled way via nitroxide exchange reaction of the nitroxide end-group on polymer chains enabling further modification and designable biointerfaces of the MOF NPs. Considering the labile nature of the nitroxide-mediated process in polymerization, our work demonstrates modulating colloidal biomolecular MOF NPs employing NMP and NER approaches, that could bring new capabilities and opportunities to explore bio-relevant applications of MOF NPs-Polymer composites.

4. Experimental Section

Materials: If not otherwise stated, materials were bought from Sigma-Aldrich and used as received. The polymers were purified by an alumina column to remove the inhibitor and stored afterward under nitrogen atmosphere in the freezer.

Characterization Techniques:

Nuclear Magnetic Resonance (NMR): ¹H and ¹³C NMR spectra in CDCl₃ were recorded on a Bruker Advanced 400 spectrometer. Chemical shifts (δ) were expressed in parts per million (ppm) referenced to the NMR solvent residual peak.

X-ray Diffraction (XRD): Powder diffraction was measured on a Bruker D8 Advance with Si strip detector (PSD Lynxeye) in - geometry at a temperature of 298K. The data were fitted by a measured Au-peak.

Dynamic Light Scattering (DLS): Particle dispersion was measured by a Zetasizer Nano ZS device from Malvern Panalytical. An EtOH and water particle suspension was used for the tests.

Scanning Electron Microscopy (ESEM): An ESEM Quattro S from ThermoScientific was used to determine the particle sizes.

The particles were dispersed into EtOH, drop cast onto a gold wafer and sputtered with a 1.5 nm gold layer using a Baltec MED-020 high-vacuum coating system.

Time-of-Flight Secondary Ion Mass Spectrometry (ToF-SIMS): ToF-SIMS was performed on a ToFSIMS5 instrument (IONTOF GmbH, Münster, Germany). The spectrometer is equipped with a Bi cluster primary ion source and a reflectron type time-of-flight analyzer. UHV base pressure during analysis was $<3 \times 10^{-8}$ mbar. For high mass resolution, the Bi source was operated in bunched mode providing short Bi_3^+ primary ion pulses at 25 keV energy, a lateral resolution of approx. 4 μm , a target current of 0.35 pA at 10 kHz repetition rate, and 1.1 ns pulse length. Data acquisition was stopped at the quasi-static limit (2×10^{11} ions per cm^2). Charge compensation was performed by applying a 21 eV electron flood gun and tuning the reflectron accordingly. Mass scale calibration was based on low Mw hydrocarbon signals together with ZrO_2^- , ZrO_3H^- , or Zr^+ signals, respectively. The primary ion beam was rastered across a $500 \times 500 \mu\text{m}^2$ field of view on the sample, and 128×128 data points were recorded.

Attenuated Total Reflection Infrared Spectroscopy (ATR-IR): A BRUKER TENSOR 27 IR Spectrometer was used for the ATR-IR measurements. The related used software was OPUS. The powder was dried under reduced pressure, and a small amount was placed on the ATR crystal for the measurement. All ATR-IR measurements were compared to pure previously produced or commercial products.

Absorbance Spectroscopy: Absorbance spectroscopy for the Proteinadsorption measurement was performed on a TECAN multimode microplate spectrometer from Spark at RT (298K). Equipped with the SparkControl Software, the absorbance was measured at 532 nm.

UiO-66-NH₂ Synthesis: The UiO-66-NH₂ particles were synthesized according to a previously described procedure.^[32] ZrCl_4 (0.240 g, 1.03 mmol) and 1.77 mL acetic acid were dissolved in 60 mL DMF by sonication for 5 min. 2-Aminotherephthalic acid (BDC-NH_2) (0.186 g, 1.03 mol) as linker was added in an equimolar ratio with regard to ZrCl_4 and dissolved by another 5 min sonication. The reaction vial was then capped, placed in an oven at 120°C, and let react for 24 h. Afterward, the synthesized nanoparticles were washed with DMF three times by centrifuging them at 8000 rpm for 10 min. Additional data supporting the chemical synthesis results is available via the Chemotion repository: <https://doi.org/10.14272/reaction/SA-FUHFF-UHFFFADPSC-YJAIWVDPLY-UHFFFADPSC-NUHFF-BUHFF-NUHFF-ZZZ>.

TEMPO-Alkoxyamine Synthesis - (4-(1-((2,2,6,6-Tetramethylpiperidin-1-yl)oxy)ethyl) Benzoic Acid): TEMPO (1 g, 6.4 mmol), 2-bromo-2-methyl propionic acid or 4-(1-bromoethyl)benzoic acid (1.2 equiv.), Cu (1.2 equiv.), CuBr (1.2 equiv.) and a stir bar were added into a three neck round flask. The flask was sealed with a rubber septum and carefully degassed and refilled with N_2 . THF (30 mL) and Bis(2-dimethylaminoethyl)methylamine (PMDETA) (2.4 equiv.) were dried separately using the freeze-pump-thaw method. THF was added in the flask, and the mixture was stirred for 10 min until the PMDETA was added. The resulting solution was subsequently stirred at room temperature for 24 h. The

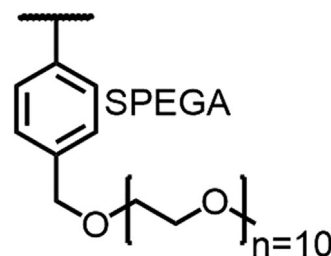


Figure 5. The used monomer for the surface modification of UiO-66-NH₂ nanoparticles: PEO-methyl-p-vinylbenzyl-ether (SPEGA).

reaction mixture was diluted with dichloromethane (DCM) (100 mL) and then washed with 5×100 mL of an aqueous disodium ethylenediamine-tetraacetate solution until the supernatant was clear, to remove the catalyst. The organic layer was dried over MgSO_4 , filtered, and evaporated. The alkoxyamines were then purified by recrystallization in MeOH under room temperature. The received product was a white/light yellow powder.^[33] (yield: 3.00 g, 3.20 mmol, 51.0 %). ^1H NMR (400 MHz, CDCl_3): δ (ppm) = 8.07 (d, J = 8.05 Hz, 2H), 7.43 (d, J = 8.0 Hz, 2H), 4.86 (q, J = 6.94 Hz, 1H), 1.50 (d, J = 6.48 Hz, 3H), 1.30-0.56 (m, 18H). ^{13}C NMR (CDCl_3): δ (ppm) = 171.77 (1C), 152.12 (1C), 130.18 (2C), 127.76 (1C), 126.59 (2C), 83.00 (1C), 59.80 (2C), 40.32 (1C), 34.19, 23.60 (2C), 20.36 (4C), 17.18 (1C). Additional data supporting the analysis of the target compound is available via the Chemotion repository: <https://doi.org/10.14272/reaction/SA-FUHFF-UHFFFADPSC-IXIHDVSFIR-UHFFFADPSC-NUHFF-NUHFF-NUHFF-ZZZ>.

Post Modification of UiO-66-NH₂ with TEMPO-Alkoxyamine: The MOF surface modification via an amide bond to the amino group of UiO-66-NH₂ was carried according to the reported literature procedure.^[15] The UiO-66-NH₂ particles (30 mg) were washed three times with EtOH and dispersed in 3 mL EtOH. Around 110 mg (0.577 mmol, 36 equiv.) of N-(3-Dimethylaminopropyl) N'-ethylcarbodiimide hydrochloride (EDC^*HCl) and a catalytic amount of N-hydroxysulfosuccinimide sodium salt (sulfo-NHS) was added. TEMPO-alkoxyamine (30 mg) was added, and the reaction was stirred overnight, washed three times with 5 mL EtOH, and stored in EtOH. Additional data supporting the chemical synthesis results is available via the Chemotion repository: <https://doi.org/10.14272/reaction/SA-FUHFF-UHFFFADPSC-ABCUGETYYU-UHFFFADPSC-NUHFF-NUHFF-NUHFF-ZZZ>.

Nitroxide-Mediated Polymerization on the MOF Surface: For the polymer grafting experiments on the MOF (UiO-66-NH₂) surface, 30 mg of the TEMPO-alkoxyamine decorated MOF particles were washed three times in 2 mL toluene and then dispersed in toluene. To this suspension, SPEGA monomers (Figure 5), and free TEMPO-alkoxyamine (30 mg) for an accelerated polymerization were added.

The reaction mixture was freeze-pump thawed three times until no further gas evolution occurs. Subsequently, the reaction mixture was placed in a preheated oil bath and stirred at 130°C for 24 h. Afterward, the mixture was cooled to room temperature to end the reaction and washed several times with 5 mL THF/EtOH (2:1) to remove the monomer and free polymer

product from the solution. The polymer grafted MOF particles were stored in EtOH and characterized according to XRD, DLS, SEM, ToF-SIMS, and ATR-IR. Additional data supporting the chemical synthesis results is available via the Chemotion repository: [https://doi.org/10.14272/reaction/SA-FUHFF-UHFFFADPSC-UHTPHSRMIL-UHFFFADPSC-NUHFF-NUHFF-ZZZ](https://doi.org/10.14272/reaction/SA-FUHFF-UHFFFADPSC-UHTPHSRMIL-UHFFFADPSC-NUHFF-NUHFF-NUHFF-ZZZ).

Protein Adsorption Test: For the Protein adsorption test 300 μg MOF nanoparticles were taken from stock and washed three times with 1 mL of a solution of 77 mg mL⁻¹ ammonium acetate (NH₄CH₃CO₂) solution in water. Then the particles were redispersed in 1 mL of 100 μg mL⁻¹ human serum albumin (HSA) solution in ammonium acetate. This procedure was conducted for the pristine and polymer-coated particles. The particle suspension was incubated at 37°C for 4 h.^[34] After incubation, the particles were centrifuged for 10 min at 10 000 rpm and the precipitates were discarded. 25 μL of the supernatant was mixed with 200 μL of the bicinchoninic acid (BCA) reagent (50:1 Regent B to A) in a 96 well plate and afterward incubated for 30 min at 37°C. The absorbance was measured at 532 nm.

RGD-Nitroxide Synthesis: In a fritted syringe, 2-chlorotriethyl chloride resin (125 mg, 200 μmol , 1.00 equiv.) was swollen in 3 mL dichloromethane (DCM) by shaking at 21 °C for at least 30 min, after completion the solvent was removed. The first amino acid (1.60 mmol, 4.00 equiv.) and N,N-diisopropylethylamine (DIPEA) (129 mg, 174 μL , 1.00 mmol, 5.00 equiv.) were dissolved in 2.5 mL dimethylformamide (DMF) and added to the resin. After shaking for 8 h, the solvent was removed, and the resin was washed with DMF, methanol, and DCM. Deprotection of the N-Fmoc-protecting group was carried out using a solution of 20% piperidine in DMF. 3 mL were added to the resin, and the mixture was left shaken for 5 min. The deprotection cocktail was removed, and the procedure was repeated twice. The resin was washed as described with DMF, methanol, and DCM. The subsequent amino acid (800 μmol , 4.00 equiv.) and O-(7-azabenzotriazol-1-yl)-N,N,N,N-tetramethyluronium-hexafluorophosphat (HATU) (306 mg, 1.60 mmol, 4.00 equiv.) were dissolved in 2.5 mL DMF, added to the loaded resin, and let shaken for 12 h. The resin was washed, deprotected, and additionally washed as described above. Coupling of amino acids (800 μmol , 4.00 equiv.), deprotection, and washing was repeated until the desired peptide was synthesized. After coupling of the last amino acid, removing the N-Alloc-protecting group was carried out using tetrakis(triphenylphosphine)palladium(0) (23.1 mg, 20.0 μmol , 0.100 equiv.) and phenyl silane (335 mg, 382 μL , 3.00 mmol, 15.0 equiv.) dissolved in dry DCM (2.5 mL). The mixture was added to the resin and was left shaking for 20 min. The procedure was repeated three times. After washing with DCM, methanol, and DMF, 3-Carboxy-2,2,5,5-tetramethylpyrrolin-1-yloxy radical (147 mg, 800 μmol , 4.00 equiv.) and HATU (306 mg, 800 μmol , 4.00 equiv.) dissolved in 2.5 mL of DMF were added to the resin, and the mixture was left shaking for 24 h. Subsequently, the N terminal Fmoc-protecting group was removed using a solution of 20% piperidine in DMF (3 x 3 mL for 5 min each). The last washing step was followed by washing with DCM (3 x 2.5 mL). Subsequently, 2.5 mL of a solution of 33% hexafluoroisopropanol in DCM was added. The resin was incubated with the cleavage cocktail twice for 1 h. The solvent was collected, and the resin was flushed with DCM five times. The solvent was removed

under an air stream resulting in the crude linear precursor. Deprotection of N-Pbf- and N-Boc-protecting group was carried out in the liquid phase. Therefore, the crude peptide was dissolved in 5 mL of 2,2,2-trifluoroacetic acid, phenol, water, and triisopropylsilane (88%:5%:5%:2% (v/v)). The mixture was stirred for 3 h. After completion, the peptide was precipitated with 15 mL of cold diethyl ether, filtered off, and washed with diethyl ether (1 x 10 mL). The desired peptide (49.8 mg, 0.08 mmol, 39%) was isolated as a white solid. MS (MALDI-TOF), m/z (%): 640 [M+H]⁺. Additional data supporting the chemical synthesis results is available via the Chemotion repository: <https://doi.org/10.14272/reaction/SA-FUHFF-UHFFFADPSC-GXXOJJSMTD-UHFFFADPSC-NUHFF-NPESU-NUHFF-ZZZ>.

Nitroxide End-Group Exchange: For the nitroxide-exchange reaction, 2 mg of the MOF-SPEGA-modified nanoparticles were dissolved in 2 mL DMF, an excess (around 1 mg) of the RGD-Nitroxide was added, and the whole mixture was freeze-pump thawed 3 times. Afterward, the reaction mixture was heated to 100°C for 24 h. After cooling to room temperature, the precipitate was washed 3 times with 1 mL DMF, and the powder sample was dried under reduced pressure for 24 h. Additional data supporting the analysis of the target compound is available via the Chemotion repository: <https://doi.org/10.14272/reaction/SA-FUHFF-UHFFFADPSC-UHFFFADPSC-UHFFFADPSC-NUHFF-NUHFF-NUHFF-ZAZ.7>.

Acknowledgements

This work was performed as part of the project "A Comprehensive Approach to Harnessing the Innovation Potential of Direct Air Capture and Storage for Reaching CO₂-Neutrality" (DACStorE), which was funded by the Initiative and Networking Fund of the Helmholtz Association (grant agreement number KA2-HSC-12). The authors thank the Institute of Functional Interfaces for the infrastructure and the financial support. Furthermore, they also thank the Carl Zeiss Foundation and the Cluster "3D Matter Made to Order" under Germany's Excellence Strategy (3DMM2O-EXC-2082-390761711, Thrust A1 and A2) for financial contributions. M.T. gratefully acknowledges the Helmholtz Association's Initiative and Networking Fund (grant VH-NG-1147) for financial support.

Conflict of Interest

The authors declare no conflict of interest.

Data Availability Statement

The data that support the findings of this study are openly available in Chemotion at <https://www.chemotion-repository.net/home/publications/collections/5728>.

Keywords

MOF nanoparticles, nitroxide exchange reaction, nitroxide-mediated polymerization, post-synthetic modification, surface functionalization

Received: February 16, 2023

Revised: March 28, 2023

Published online:

- [1] H. Furukawa, K. E. Cordova, M. O'Keeffe, O. M. Yaghi, *Science* **2013**, 341, 1230444.
- [2] S. Kitagawa, R. Kitaura, S.-i. Noro, *Angew. Chem. Int. Ed.* **2004**, 43, 2334.
- [3] G. Férey, *Chem. Soc. Rev.* **2008**, 37, 191.
- [4] S. Wang, C. M. McGuirk, A. d'Aquino, J. A. Mason, C. A. Mirkin, *Adv. Mater.* **2018**, 30, 1800202.
- [5] E. Ploetz, H. Engelke, U. Lächelt, S. Wuttke, *Adv. Funct. Mater.* **2020**, 30, 1909062.
- [6] B. V. Schmidt, *Macromol. Rapid Commun.* **2020**, 41, 1900333.
- [7] T. Simon-Yarza, A. Mielcarek, P. Couvreur, C. Serre, *Adv. Mater.* **2018**, 30, 1707365.
- [8] P. Horcajada, T. Chalati, C. Serre, B. Gillet, C. Sebrie, T. Baati, J. F. Eubank, D. Heurtaux, P. Clayette, C. Kreuz, J.-S. Chang, Y. K. Hwang, V. Marsaud, P.-N. Bories, L. Cynober, S. Gil, G. Férey, P. Couvreur, R. Gref, *Nat. Mater.* **2010**, 9, 172.
- [9] P. Horcajada, R. Gref, T. Baati, P. K. Allan, G. Maurin, P. Couvreur, G. Férey, R. E. Morris, C. Serre, *Chem. Rev.* **2012**, 112, 1232.
- [10] R. S. Forgan, *Dalton Trans.* **2019**, 48, 9037.
- [11] T. Kitao, Y. Zhang, S. Kitagawa, B. Wang, T. Uemura, *Chem. Soc. Rev.* **2017**, 46, 3108.
- [12] K. Lu, T. Aung, N. Guo, R. Weichselbaum, W. Lin, *Adv. Mater.* **2018**, 30, 1707634.
- [13] S. Wang, S. S. Park, C. T. Buru, H. Lin, P.-C. Chen, E. W. Roth, O. K. Farha, C. A. Mirkin, *Nat. Commun.* **2020**, 11, 1.
- [14] A. Zimpel, N. Al Danaf, B. Steinborn, J. Kuhn, M. Höhn, T. Bauer, P. Hirschle, W. Schrimpf, H. Engelke, E. Wagner, M. Barz, D. C. Lamb, U. Lächelt, S. Wuttke, *ACS Nano* **2019**, 13, 3884.
- [15] A. Zimpel, T. Preiß, R. Roder, H. Engelke, M. Ingrisch, M. Peller, J. O. Radler, E. Wagner, T. Bein, U. Lächelt, S. Wuttke, *Chem. Mater.* **2016**, 28, 3318.
- [16] S. Yang, V. V. Karve, A. Justin, I. Kochetygov, J. Espin, M. Asgari, O. Trukhina, D. T. Sun, L. Peng, W. L. Queen, *Coord. Chem. Rev.* **2021**, 427, 213525.
- [17] M. Kalaj, S. M. Cohen, *ACS Cent. Sci.* **2020**, 6, 1046.
- [18] M. Sindoro, N. Yanai, A.-Y. Jee, S. Granick, *Acc. Chem. Res.* **2014**, 47, 459.
- [19] M. Fang, J. Cambedouzou, D. Cot, C. Gomri, S. Nehache, C. Montoro, M. Semsarilar, *J. Membr. Sci.* **2022**, 657, 120669.
- [20] S. Spiegel, I. Wagner, S. Begum, M. Schwotzer, I. Wessely, S. Bräse, M. Tsotsalas, *Langmuir* **2022**, 38(21), 6531–6538.
- [21] K. A. McDonald, J. I. Feldblyum, K. Koh, A. G. Wong-Foy, A. J. Matzger, *Chem. Commun.* **2015**, 51, 11994.
- [22] M. Kalaj, K. C. Bentz, S. Ayala Jr, J. M. Palomba, K. S. Barcus, Y. Katayama, S. M. Cohen, *Chem. Rev.* **2020**, 120, 8267.
- [23] S. Hansson, V. Trouillet, T. Tischer, A. S. Goldmann, A. Carlmark, C. Barner-Kowollik, E. Malmstrom, *Biomacromolecules* **2013**, 14, 64.
- [24] Y. Jia, G. Delaittre, M. Tsotsalas, *Macromol. Mater. Eng.* **2022**, 307, 2200178.
- [25] Y. Jia, C. A. Spiegel, A. Welle, S. Heißler, E. Sedghamiz, M. Liu, W. Wenzel, M. Hackner, J. P. Spatz, M. Tsotsalas, E. Blasco, *Adv. Funct. Mater.* **2022**, 2207826.
- [26] L. Tebben, A. Studer, *Angew. Chem. Int. Ed.* **2011**, 50, 5034.
- [27] D. Bertin, D. Gigmès, S. R. Marque, P. Tordo, *Chem. Soc. Rev.* **2011**, 40, 2189.
- [28] J. P. Blinco, K. E. Fairfull-Smith, A. S. Micallef, S. E. Bottle, *Polym. Chem.* **2010**, 1, 1009.
- [29] Y. Jia, Y. Matt, Q. An, I. Wessely, H. Mutlu, P. Theato, S. Bräse, A. Llevot, M. Tsotsalas, *Polym. Chem.* **2020**, 11, 2502.
- [30] I. Wessely, V. Mugnaini, A. Bihlmeier, G. Jeschke, S. Bräse, M. Tsotsalas, *RSC Adv.* **2016**, 6, 55715.
- [31] E. Ruoslahti, M. D. Pierschbacher, *Science* **1987**, 238, 491.
- [32] A. Schaate, P. Roy, A. Godt, J. Lippke, F. Waltz, M. Wiebcke, P. Behrens, *Chem. Eur. J.* **2011**, 17, 6643.
- [33] D. Le, T. N. T. Phan, L. Autissier, L. Charles, D. Gigmès, *Polym. Chem.* **2016**, 7, 1659.
- [34] X. Li, G. Salzano, J. Qiu, M. Menard, K. Berg, T. Theodossiou, C. Ladavière, R. Gref, *Front. Bioeng. Biotechnol.* **2020**, 8, 1027.